ESMO GOOD SCIENCE BETTER MEDICINE BEST PRACTICE

ANNALS OF ONCOLOGY driving innovation in oncology

ORIGINAL ARTICLE

# Prediction of response to immune checkpoint blockade in patients with metastatic colorectal cancer with microsatellite instability

T. Ratovomanana[1†], R. Nicolle[2,3†], R. Cohen[1,3,4], A. Diehl[1], A. Siret[1], Q. Letourneur[1], O. Buhard[1], A. Perrier[1,5], E. Guillerm[1,5], F. Coulet[1,5], P. Cervera[1], P. Benusiglio[1,5], K. Labrèche[6], R. Colle[1,3,4], A. Collura[1], E. Despras[1], P. Le Rouzic[1], F. Renaud[1], J. Cros[7], A. Alentorn[8], M. Touat[8], M. Ayadi[9], P. Bourgoin[1,10], C. Prunier[11], C. Tournigand[12], C. de la Fouchardière[13], D. Tougeron[14], V. Jonchère[1], J. Bennouna[15], A. de Reynies[16], J.-F. Fléjou[1,10], M. Svrcek[1,10], T. André[1,3,4] & A. Duval[1,5*‡]

[1]Sorbonne Université, INSERM, Unité Mixte de Recherche Scientifique 938 and SIRIC CURAMUS, Centre de Recherche Saint-Antoine, Equipe Instabilité des Microsatellites et Cancer, Equipe labellisée par la Ligue Nationale contre le Cancer, Paris; [2]Université Paris Cité, Centre de Recherche sur l'Inflammation (CRI), INSERM, U1149, CNRS, ERL 8252, Paris; [3]GERCOR, Groupe Coopérateur Multidisciplinaire en Oncologie, Paris; Departments of [4]Medical Oncology; [5]Molecular Biology and Medical Genetics, Sorbonne Université, AP-HP, Hospital Pitié-Salpêtrière, Paris; [6]CinBioS, MS 37 PASS Production de données en Sciences de la vie et de la Santé, INSERM, Sorbonne Université et SIRIC CURAMUS, Paris; [7]Department of Pathology, Beaujon Hospital, AP-HP, Clichy; [8]Service de Neurologie 2-Mazarin, Sorbonne Université, Inserm, CNRS, UMR S 1127, Institut du Cerveau, ICM, AP-HP, Hôpitaux Universitaires La Pitié Salpêtrière—Charles Foix, 47-83 boulevard de l'Hôpital, Paris; [9]Programme "Cartes d'Identité des Tumeurs", Ligue Nationale Contre le Cancer, Paris; [10]Department of Pathology, Sorbonne Université, AP-HP, Hôpital Saint-Antoine, Paris; [11]Sorbonne Université, INSERM, Unité Mixte de Recherche Scientifique 938 and SIRIC CURAMUS, Centre de Recherche Saint-Antoine, Equipe Signalisation TGFB, plasticité cellulaire et Cancer, Paris; [12]Department of Medical Oncology, Hôpital Henri-Mondor, APHP, Université Paris Est Creteil, INSERM U955, Créteil; [13]Department of Medical Oncology, Centre Léon Bérard, Lyon; [14]ProDicET, UR 24144, University of Poitiers and Hepato-Gastroenterology Department, Poitiers University Hospital, Poitiers; [15]Centre De Recherche En Cancérologie Et Immunologie Nantes-Angers (CRCINA), INSERM, Université d'Angers, Université De Nantes, Nantes; [16]Cartes d'Identité des Tumeurs Program, Ligue Nationale Contre Cancer, Paris, France

Available online 1 June 2023

**Background:** Mismatch repair-deficient (dMMR) tumors displaying microsatellite instability (MSI) represent a paradigm for the success of immune checkpoint inhibitor (ICI)-based immunotherapy, particularly in patients with metastatic colorectal cancer (mCRC). However, a proportion of patients with dMMR/MSI mCRC exhibit resistance to ICI. Identification of tools predicting MSI mCRC patient response to ICI is required for the design of future strategies further improving this therapy.

**Patients and methods:** We combined high-throughput DNA and RNA sequencing of tumors from 116 patients with MSI mCRC treated with anti-programmed cell death protein 1 ± anti-cytotoxic T-lymphocyte-associated protein 4 of the NIPICOL phase II trial (C1, NCT03350126, discovery set) and the ImmunoMSI prospective cohort (C2, validation set). The DNA/RNA predictors whose status was significantly associated with ICI status of response in C1 were subsequently validated in C2. Primary endpoint was progression-free survival by immune RECIST (iRECIST) (iPFS).

**Results:** Analyses showed no impact of previously suggested DNA/RNA indicators of resistance to ICI, e.g. MSIsensor score, tumor mutational burden, or specific cellular and molecular tumoral contingents. By contrast, iPFS under ICI was shown in C1 and C2 to depend both on a multiplex MSI signature involving the mutations of 19 microsatellites hazard ratio cohort C2 ($HR_{C2}$) = 3.63; 95% confidence interval (CI) 1.65-7.99; $P = 1.4 \times 10^{-3}$] and the expression of a set of 182 RNA markers with a non-epithelial transforming growth factor beta (TGFB)-related desmoplastic orientation ($HR_{C2} = 1.75$; 95% CI 1.03-2.98; $P = 0.035$). Both DNA and RNA signatures were independently predictive of iPFS.

**Conclusions:** iPFS in patients with MSI mCRC can be predicted by simply analyzing the mutational status of DNA microsatellite-containing genes in epithelial tumor cells together with non-epithelial TGFB-related desmoplastic RNA markers.

**Key words:** metastatic colorectal cancer, microsatellite instability, immune checkpoint inhibitors (ICIs), DNA and RNA sequencing, prediction of MSI mCRC patient response to ICI, progression-free survival by iRECIST

## INTRODUCTION

Mismatch repair-deficient (dMMR) tumors display a molecular phenotype characterized by the genetic instability of numerous microsatellite repeated sequences throughout the genome [microsatellite instability (MSI)].[1-3] MSI was first observed in inherited tumors associated with Lynch

*Correspondence to: Prof. Alex Duval, Team "Microsatellite Instability and Cancer", Inserm UMRS 938, CRSA, Sorbonne University, Hôpital Saint-Antoine, Paris 75010, France. Tel: 00331 49 28 66 80
E-mail: alex.duval@inserm.fr (A. Duval).

†Co-first authors.
‡Leadership.

syndrome and later in a large spectrum of primary tumors, in particular sporadic colorectal cancers (CRCs).[4-6] Being highly genetically unstable, MSI cancers are highly immunogenic and generally show a strong infiltration with cytotoxic T-cell lymphocytes (CTLs).[4] Recently, it was reported that MSI tumors resist this hostile immune microenvironment by overexpressing immune checkpoint (ICK)-related proteins to allow immune escape.[7] Consistently, MSI status was shown to predict clinical benefit from ICK inhibitors (ICI) in patients with metastatic cancer including CRC (mCRC).[8,9] In patients pretreated with fluoropyrimidines, oxaliplatin, and irinotecan before ICI for dMMR/MSI mCRC, the objective response rate ranges from 33% to 65% and the 1-year overall survival rate ranges from 34% to 71%. First-line pembrolizumab [anti-programmed cell death protein 1 (PD-1)] has been associated with significant improvement of progression-free survival (PFS) compared with standard-of-care chemotherapy ± cetuximab or bevacizumab.[10] However, up to 15%-46% of patients with dMMR/MSI mCRC exhibit primary resistance to ICI while 5%-25% of responders develop acquired resistance to these treatments, although this estimation might increase with longer follow-up.[11-14]

Several DNA and RNA-based markers predicting the efficacy of ICIs have been previously proposed in metastatic dMMR/MSI cancer settings.[9,15-21] However, it is fair to say that these results lack independent validation, being based on the analysis of only limited series of dMMR/MSI tumor samples with heterogeneous tumor origins. At the DNA level, markers include quantitative genomic indexes measuring the level of MSI within the tumor bulk such as the MSIsensor score or the tumor mutation burden (TMB). Previous studies have considered the selection of specific somatic variants occurring in dMMR cancers due to MSI as specific predictive markers such as *BRAF*$^{V600E}$ mutational status, *KRAS*/*NRAS* mutations, or the *B2M* truncating mutation resulting in loss of function of the resultant protein were associated with the major histocompatibility complex class I.[17,20] However, it was recently reported that B2M inactivation was unlikely to blunt the efficacy of ICI in dMMR/MSI tumors in human[22] and using multiple murine dMMR B2m null cancer models,[23] raising the question of the real impact of these somatic mutations in the MSI cancer setting. At the RNA level, it was hypothesized that the estimated abundance of specific cell populations in the tumor microenvironment could be of clinical relevance, e.g. immune cell populations such as antigen-presenting macrophages interacting with T cells.[20] Logically, deregulated activity of some cancer-related pathways associated with antitumor immunity was also proposed, e.g. the reduced activity of Wnt/Wingless signaling, deregulation of the interferon-γ pathway and/or of several immune escape processes.[20] Finally, a study published by our team showed that the leading cause for association of primary resistance to ICI in mCRC was the misdiagnosis of their MSI or dMMR status,[24] emphasizing that the first and foremost criterion to be validated before the prescription of ICI in metastatic dMMR/MSI cancer patients, and particularly in mCRC, is the guarantee of a quality diagnosis with appropriate methods to identify genuine dMMR/MSI.

In this study, we hypothesized that the response to ICI could be predicted by both levering on the MSI-specific mutational patterns in epithelial cells (by DNA sequencing) and by considering the modifications of the cancer stroma [by RNA sequencing (RNASeq)] on the other hand. We addressed the issue of response to ICI, using a discovery and validation strategy, on the investigation of two independent prospective cohorts of 44 and 72 patients with dMMR/MSI mCRC, respectively, in the multicentric NIPICOL clinical trial (NCT03350126)[14] and the prospective ImmunoMSI cohort.[25]

## PATIENTS AND METHODS

### Patients

The NIPICOL clinical trial (C1) was conducted in accordance with the tenets of the Declaration 170 of Helsinki and Good Clinical Practice Guidelines, after approval by the ethics board, and was registered at ClinicalTrials.gov (clinical trial number: NCT03350126). Written informed consent was obtained from all patients. All patients included in C1 received anti-PD-1 (nivolumab) + anti-CTL4 (ipilimumab). Concerning ImmunoMSI prospective cohort (C2),[25] all consecutive MSI/dMMR mCRC patients treated with ICI [anti-PD-1 monotherapy or anti-PD-1 plus anti-cytotoxic T-lymphocyte-associated protein 4 (CTLA-4) combination] at Saint-Antoine Hospital, Medical Oncology department (Prof. T. André) from February 2015 to December 2019 were included. This research was approved by the ethics committee (N°2020—CER 2020-6). The identification numbers of the ethics committees are as follows: CPP N°2017/45 (ANSM reference: 170508A-12; EudraCT N°2017-002442-72) for C1 NIPICOL clinical trial and CPP N°2020 CER 2020-6C2 for ImmunoMSI. The NIPICOL trial NCT03350126 has been completed and its primary endpoint published.[14]

### Assessment of microsatellite status

All CRC samples from C1, C2, and other cohorts used in this *post hoc* study were centrally reassessed for MSI and dMMR status using immunohistochemistry (IHC) and for MSI using PCR as described.[26,27] Next, MSIsensor (version 0.6) and MSICare were used by default on paired normal-tumor exome data, to evaluate the mutation status of microsatellites using the whole exome data. An MSIsensor score threshold of 10% or more was used to classify the MSI-H tumor (MSI-high) and an MSICare threshold of 20% was used to define MSI status as previously described.[28]

### Radiological analyses

Tumors were assessed ≤28 days before the first dose (baseline) and every 6-10 weeks, thereafter, according to different protocols. The decision to pursue treatment beyond unconfirmed progression disease by iRECIST (iuPD) was at the discretion of the treating physician. Treatment beyond iuPD was conditional to a confirmatory imaging 4-8 weeks after the first evidence of progression. Imaging was retrospectively and centrally reviewed by an experienced

radiologist according to RECIST1.1 and immune RECIST (iRECIST).[29] Radiological progression was defined as confirmed progressive disease (cPD) according to iRECIST. All cases of PD and pseudoprogression were reviewed by a second experienced radiologist unaware of the target and non-target lesions chosen by the first radiologist. In case of discrepancy, a final decision was reached by consensus.

### Survival analysis of ICI-treated patients

Survival analysis on ICI patients was carried out from the date of first infusion of any ICI. PFS by iRECIST (iPFS)[29] was calculated from the first dose to the first documented cPD, or death resulting from any cause, whichever occurred first. Kaplan–Meier curves were used to visualize difference in PFS (iPFS) between patients' groups diverging on genomic instability (e.g. TMB-high or MSIsensor-high or MSICare-high, >10th percentile; TMB-low or MSIsensor-low or MSICare-low, ≤10th percentile) or to show at the selected cut-off values a clinical effect of our DNA or RNA signatures. The cut-off values were selected to optimize the clinical effect of our DNA or RNA signatures on ICI response in patients. Nevertheless, the validity of same signatures was also tested without using cut-off values with Cox models, similarly showing a clinical relevance, as indicated in the corresponding figures. The use of the cut-offs has been envisioned more to illustrate the findings but there is no dependence on these cut-offs for the demonstration of the clinical impact of both the DNA and RNA signatures. Two-sided log-rank test was carried out using the R package Survival (version 3.2.3; Nanostring, Seattle, WA).

### P value levels and correction of P values

In all statistical analyses, *P* value ≤0.05 (risk α) was used as a threshold of significance. As an exception, for the selection of DNA variants following whole exome sequencing (WES) in C1, *P* value ≤0.1 has been applied in order to provide pre-selection of a larger number of DNA variants before validation of their putative clinical significance in C2 by targeted sequencing (reduction of the risk of false negatives).

We systematically applied multi-test correction using Benjamini–Hochberg's method to control the false discovery rate when multiple tests of the same hypotheses were carried out. However, we chose to highlight either one or the other either for clarity or fairness of comparison. We systematically presented uncorrected and corrected *P* values when relevant in each of the corresponding figures and Supplementary Figures, available at https://doi.org/10.1016/j.annonc.2023.05.010.

### Data availability

The processed datasets used in the current study are now available in the GitHub repository, https://github.com/CRSA-MSI/R-ICI_MNB_Survival. Reasonable request for sharing biologic materials or raw data files will be reviewed by the corresponding author (ADu). Patient-related data not included in the paper were generated as part of clinical trials and may be subject to patient confidentiality. Any data and materials that can be shared will be released via a material transfer agreement.

### Code availability

The scripts and the naive Bayes model can be accessed at GitHub https://github.com/CRSA-MSI/R-ICI_MNB_Survival. Scripts for ICA of RNA can be accessed at GitHub https://github.com/GeNeHetX/NipicolICA.

Concerning sample preparation and sequencing, exome analysis and mutational load, feature selection and data preprocessing, DNA signatures (mutation count and multinomial naive Bayes), and transcriptome profile generation and analysis, see Supplementary Materials and Methods, available at https://doi.org/10.1016/j.annonc.2023.05.010. See also Supplementary Materials and Methods, available at https://doi.org/10.1016/j.annonc.2023.05.010, for the statistical reporting which explains in detail the methodology that was used to identify and validate innovative DNA and RNA signatures predictive of MSI mCRC patient response to ICI.

## RESULTS

### Patient population and study design

A total of 129 prospectively collected mCRC patients were assessed for eligibility, including 57 patients from the NIPICOL clinical trial (C1, NCT03350126) and 72 patients from the prospective ImmunoMSI cohort (C2).[25] Clinical and disease characteristics of patients from C1 and C2 are summarized in Table 1, and further detailed in Supplementary Tables S1 and S2, available at https://doi.org/10.1016/j.annonc.2023.05.010. In C1, the selection for analysis was applied to 54 MSI mCRC patients and 3 mCRC samples with misdiagnosed dMMR/MSI status (false-positive cases) that were in fact MSS. WES and RNASeq were carried out on 23 and 44 collected MSI mCRC ± matched normal colonic mucosa paraffin-embedded samples, respectively, after removing 29 samples with lack of materials and/or insufficient quality (Figure 1A). In C2, targeted next-generation sequencing (NGS) was carried out on 66 mCRC ± matched normal colonic mucosa paraffin-embedded samples of which 35 were also sequenced more widely by WES. RNASeq was carried out on 72 mCRC after removing unqualified samples for similar reasons, i.e. insufficient quantity and/or low-quality level (Figure 1A). Apart from the quality and/or quantity of the DNA/RNA material, we worked without any other selection criteria. The Consolidated Standards of Reporting Trials (CONSORT)-like clinical and molecular diagram in Figure 1 outlines the methodology workflow of the study. Finally, a subset of 96 tumor samples from C1 ($n = 27$) and C2 ($n = 69$) were again assessed by a nanoString nCounter® RNA technology (Nanostring) more accessible for routine clinical practice.

Figure 1 also summarizes the flow chart (Figure 1A) and the current design of the study (Figure 1B). In brief, NIPICOL (C1) was used as a training cohort and ImmunoMSI (C2) as a validation cohort. iPFS[29] was used as primary endpoint. In an effort to optimize the available clinical data for the

**Table 1. Patients' description from cohort 1 (C1) and cohort 2 (C2) with main corresponding clinical data**

| Characteristic | ImmunoMSI, $n = 72$[a] | NIPICOL, $n = 47$[a] | $P$ value[b] |
|---|---|---|---|
| Age in **ye**ars | 59 (15) | 54 (13) | 0.058 |
| Sex | | | 0.87 |
| Female/**m**ale | 28/44 | 19/28 | |
| ECOG performance score | | | 0.24 |
| 0/≥1/**u**nknown | 35/36/1 | 18/29/0 | |
| Primary tumor location | | | 0.49 |
| Left colon/**r**ight colon/**u**nknown | 23/47/2 | 18/28/1 | |
| BRAFV600E | | | 0.056 |
| Mutated/**w**ild type/**u**nknown | 23/49/0 | 7/37/3 | |
| KRAS | | | 0.029 |
| Mutated/**w**ild type | 21/51 | 23/24 | |
| NRAS | | | >0.99 |
| Mutated/**w**ild type/**u**nknown | 1/71/0 | 1/42/4 | |
| Origin of MMR deficiency | | | 0.82 |
| Known germline mutation | 20 | 27 | |
| Sporadic/**u**nknown | 10/42 | 12/8 | |
| Surgery of primary tumor | | | >0.99 |
| Yes/no/**u**nknown | 71/1/0 | 43/1/3 | |
| Number of metastatic sites | | | 0.50 |
| 1/2/≥3 | 27/26/19 | 14/18/15 | |
| Number of prior lines | | | 0.006 |
| 0/1/2/≥3 | 9/21/32/10 | 0/8/22/17 | |
| Type of immunotherapy | | | <0.001 |
| Anti-PD-1/anti-PD-1 **and** CTLA-4 | 43/29 | 0/47 | |
| iRECIST | | | <0.001 |
| CR/PR/SD/PD/NE | 20/35/7/8/2 | 2/15/24/3/3 | |
| Status | | | 0.059 |
| MSI/MSS | 72/72 (100) | 44/3 | |

CR, complete response; CTLA-4, cytotoxic T-lymphocyte-associated protein 4; ECOG, Eastern Oncology Cooperative Group; iRECIST, immune RECIST; MMR, mismatch repair; MSI, microsatellite instability; MSS, microsatellite stable, NE, not evaluable; PD, progressive disease; PD-1, programmed cell death protein 1; PR, partial response; SD, stable disease.
[a]Mean (standard deviation); *n*/*N* (%).
[b]Wilcoxon rank sum test; Pearson's chi-square test; Fisher's exact test.

purpose of identifying available RNA/DNA predictive markers of resistance to ICI in this prospective series of ICI-treated patients with MSI mCRC, their putative clinical relevance was examined in C1 (training set) and in C2 (validation set) independently. C1 was a cohort from a clinical trial including dMMR/MSI patients all treated with the same treatment, i.e. a combination of nivolumab (anti-PD-1) and ipilimumab (anti-CTLA-4) after failure of standards of care. C2 was a larger and more heterogeneous cohort concerning regimen of ICI received (anti-PD-1 alone or associated with ipilimumab) and inclusion criteria were less restrictive compared to a clinical trial. We checked that the C1 population of this ancillary study is fully representative of the full population of the NIPICOL trial without introducing any population bias with respect to important clinical and biological criteria (see Supplementary Table S3, available at https://doi.org/10.1016/j.annonc.2023.05.010). Regarding the C2 cohort (ImmunoMSI), it is a prospective cohort for which the absence of available tumor material was not an exclusion criterion.

### *The level of MSI and TMB in tumor DNA does not predict response to ICI in patients with ICI-treated MSI mCRC following necessary exclusion of ICI-treated mCRC with misdiagnosed dMMR/MSI status which are pitfalls for the correct estimation of these genomic indexes*

We first focused DNA analyses on quantitative genomic instability indexes, i.e. the TMB and MSIsensor score, whose level was previously reported to predict response to ICI in patients with metastatic dMMR tumor.[15,16] Regardless of the cut-off selected for these indexes, our data show no influence of MSIsensor score or TMB on the iPFS of patients from C1 (after exclusion of the cases with false-positive MSI status that were MSS, $n = 3$ and may lead to wrongly give a prognostic value to TMB and/or MSIsensor regarding iPFS) (Figure 2A and Supplementary Figure S1A, available at https://doi.org/10.1016/j.annonc.2023.05.010).[30-33] Since these results are discordant with others in the field, we sought to confirm them in the C2 cohort in the 35 patients for whom WES was carried out (Figure 1A). Similar analyses were carried out and confirmed at multiple cut-offs for the same negative results (Supplementary Figure S1A, available at https://doi.org/10.1016/j.annonc.2023.05.010).

Next, we found of interest to further conduct similar investigations at multiple cut-offs with inclusion of diagnostic errors on the MSI status of tumors (i.e. inclusion of three false-positive MSI cases from the C1 NIPICOL trial; cf. Cohen et al.[24]). We had enough power to conclude that accounting for these MSI misdiagnoses drastically changes the predictive value of TMB and MSIsensor at the 10% threshold (10th percentile), leading to a significant false ability of these genomic indexes to predict ICI resistance at this low cut-off for the TMB and for MSIsensor (Figure 2A and Supplementary Figure S1B, available at https://doi.org/10.1016/j.annonc.2023.05.010). As shown also in Supplementary Figure S1C, available at https://doi.org/10.1016/j.annonc.2023.05.010,

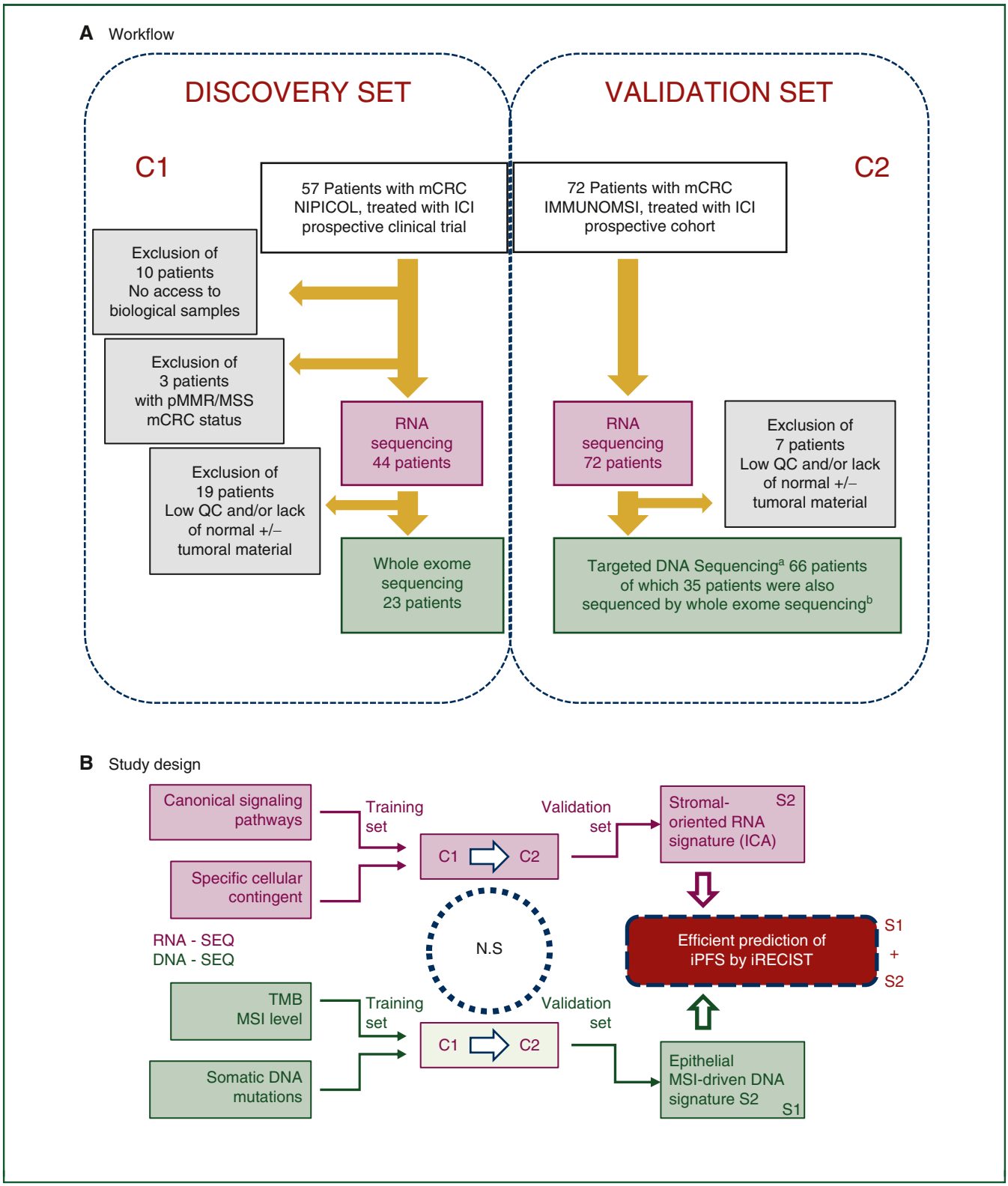


**Figure 1. Workflow and study design.**
ICI, immune checkpoint inhibitors; IHC, immunohistochemistry; mCRC, metastatic colorectal cancer; MSI, microsatellite instability; MSS, microsatellite stable; pMMR, mismatch repair proficient; QC, quality control; TMB, tumor mutation burden; WES, whole exome sequencing.
[a]Targeted sequencing of 362 somatic variants in C2 associated to resistance to treatment in C1.
[b]WES to re-analyze TMB, MSIsensor, and MSICare in C2 as in C1.

similar results were obtained using the MSICare score. All these results obtained for TMB, MSIsensor, and MSICare scores in association with iPFS to ICI in C1 and/or C2 before or after removing false MSI-positive cases are shown in Supplementary Table S4, available at https://doi.org/10.1016/j.annonc.2023.05.010.

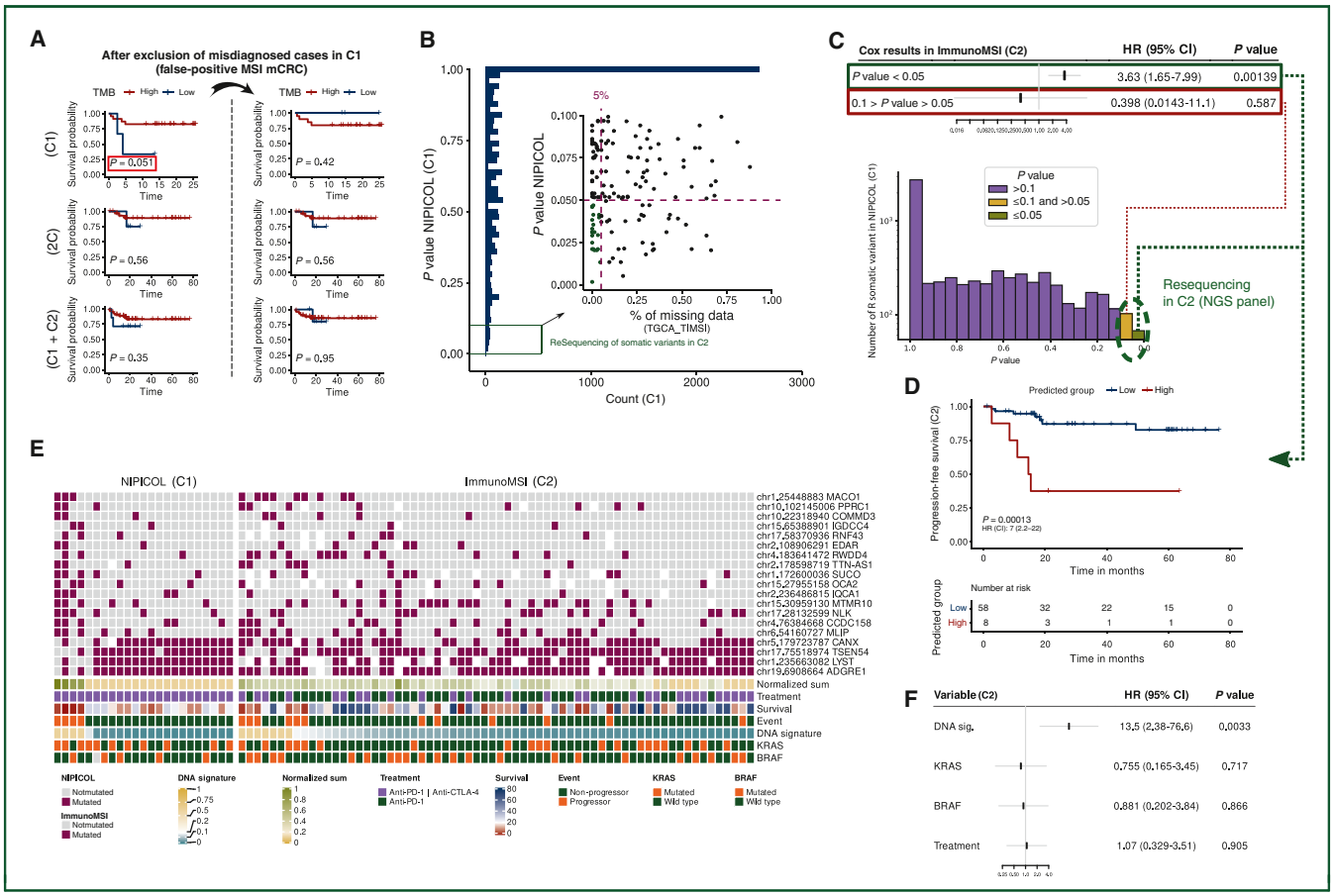


**Figure 2. Identification of a 19-plex MSI signature predictive of response to ICI in mCRC patients.** (A) Kaplan−Meier curves of progression-free survival (iPFS) for tumor mutation burden (TMB) and MSIsensor score in the NIPICOL cohort (C1), the ImmunoMSI cohort (C2), and the combined dataset (C1 + C2). The cohorts (C1, C2, and C1 + C2) were stratified into distinct groups using a 10th percentile cut-off (low, individuals with TMB or MSIsensor score at or below the 10th percentile; high, individuals with TMB or MSIsensor score above the 10th percentile). (B) Histogram displaying the *P* values obtained from Cox analysis for repeat variants (microsatellites) in the C1 NIPICOL cohort. A zoom was carried out on those having a *P* value <0.1 ($n = 167$). The 19 somatic microsatellite variants with a known percentage of missing data <5% in the C1 cohort as well as other public and private cohorts are indicated in green. These variants were further investigated to assess their impact on progression-free survival (iPFS) in the C2 cohort. (C) Counts of somatic microsatellite variants according to their *P* value obtained from the univariate Cox regression model on the 23 patients of NIPICOL cohort (C1). Green and red bars represent the mutated microsatellites with a *P* value <0.05 and $0.05 \leq P$ value < 0.1, respectively. The top forest plot represents the results of Cox survival regression analysis on the prediction of risk output in the C2 cohort The risk output is indicated by the hazard ratio (HR), where HR <1 denotes a beneficial effect, HR = 1 indicates no effect, and HR >1 signifies a deleterious effect. The features selected for Cox analysis are distinguished by their significance levels: high stringency ($P < 0.05$, DNA signature) is depicted in green, while low stringency based on *P* value is shown in red. (D) Kaplan−Meier curves illustrating progression-free survival (iPFS) based on the risk probability in the ImmunoMSI cohort (C2, $n = 66$). Red curve corresponds to patients with high naive Bayes (NB) probability (>20%), while the blue curve corresponds to patients with low NB probability (≤20%). (E) Heatmap representation of the NIPICOL cohort (C1) and ImmunoMSI cohort (C2). Overview of mutation profile for each patient in relation to the list of 19 selected microsatellites (MS). The genes' name and chromosomal location are indicated on the right side of the heatmap. The bottom bars in the heatmap represent additional patient information, including their treatment (combo-therapy or monotherapy), survival (time to event), event (progressor or non-progressor), DNA signature (probability of non-response based on iPFS as determined by the NB), and KRAS and BRAF mutational status. Patients are ordered based on their predicted risk of progression and the MS are ordered based on their mutation frequency in the NIPICOL cohort. (F) Forest plot presenting the results of the multivariate Cox regression analysis with progression-free survival (iPFS) in cohort C2. The forest plot displays the HR and their corresponding *P* values. The included features in the analysis are DNA signature (low to high risk), BRAF, KRAS (wild type versus mutated status), and treatment (mono versus combo).
ICI, immune checkpoint inhibitor; iPFS, progression-free survival by immune RECIST; mCRC, metastatic colorectal cancer; MSI, microsatellite instability; PD-1, programmed cell death protein 1.

### *Identification of a 19-plex MSI signature predictive of response to ICI in MSI mCRC patients*

We first examined by WES the impact of somatic variants occurring in true-positive MSI mCRC patients from C1 regarding iPFS upon ICI treatment. Expectedly, a great number of variants occurred at both nonrepetitive (NR, in $n = 3886$ genes, only coding events) and repetitive (R, in $n = 20\,472$ microsatellite-containing genes, both coding and noncoding events) sequences in genes having or not an expected role in the MSI-driven tumorigenic process. For survival analyses, we considered only somatic microsatellite mutations in tumor DNAs, because frequent hotspot NR mutations are rare in these tumors (Figure 2B and C). However, note that canonic NR mutations recurrently associated with colon tumor among which some were previously proposed to affect response to ICI, e.g. in *KRAS*, *BRAF*, *B2M*, and other cancer-related genes including genes with somatic mutations putatively influencing immune response in MSS digestive tumors,[34] were checked as not being associated with shorter iPFS (Supplementary

Figure S2, available at https://doi.org/10.1016/j.annonc.2023.05.010). Figure 2C shows the results of univariate Cox analyses we carried out to identify amongst the microsatellite variants the 167 alterations with impact on the iPFS of MSI mCRC patients in C1 ($P \leq 0.1$).

Like the NGS-based MSICare[28] or the PCR Pentaplex[26] genomic tools we previously designed, which use multiple microsatellite analysis to predict the MSI or MSS status of CRC, we hypothesized that response to ICI could be also predicted by investigating a set of selected microsatellite markers mutated in these tumors. From C1 (training cohort), 19 candidate microsatellite markers (i.e. in *SUCO*, *LYST*, *MACO1*, *PPRC1*, *COMMD3*, *OCA2 MTMR10*, *IGDCC4*, *NLK*, *RNF43*, *TSEN54*, *ADGRE1*, *EDAR*, *TTN-AS1*, *IQCA1*, *RWDD4*, *CCDC158*, *CANX*, *MLIP*) were selected since: (i) their somatic mutations were each associated with iPFS in C1 ($\alpha = 5\%$) (Figure 2B and Supplementary Table S5, available at https://doi.org/10.1016/j.annonc.2023.05.010) and (ii) their sequencing in C1 but also in additional public (Colorectal Adenocarcinoma from The Cancer Genome Atlas) and private cohorts using NGS was successful in at least 95% of tumors (Figure 2B and Supplementary Table S5, available at https://doi.org/10.1016/j.annonc.2023.05.010) or, in other words, that these loci were particularly easy to analyze which is not always the case especially for microsatellite markers. A predictive nature of this 19-plex identified DNA signature based on the concomitant analysis of their microsatellite somatic variations in tumor DNA as compared to matched normal DNA, which was then evaluated by simply calculating for each patient the mean count of all the mutations in those microsatellites, with a significant association to iPFS in C2 [Cox regression on the continuous values: hazard ratio cohort C2 ($HR_{C2}$) = 4.37; 95% confidence interval (CI) 1.41-13.6; $P = 1 \times 10^{-2}$] (see in Figure 2C and Supplementary Figure S3, available at https://doi.org/10.1016/j.annonc.2023.05.010, the validation of this DNA signature regarding iPFS to ICI in C2). We also trained a naive Bayes (NB) classifier as a simple machine learning method to predict the risk of progression with the 19-plex signature.[35] We trained the NB method on NIPICOL (C1) and validated it on ImmunoMSI (C2). Applying the trained model in C2 (validation cohort), we were able to show using NB that the same 19-plex MSI signature was even more significantly associated to iPFS ($HR_{C2} = 3.63$; 95% CI 1.65-7.99; $P = 1.3 \times 10^{-4}$) (Figure 2D). Figure 2 further illustrates how the 19 microsatellite mutations contribute to predicting resistance to ICI in MSI mCRC patients (see the heatmap in Figure 2E). In the multivariate analysis we conducted in C2 including molecular and clinical data (e.g. *KRAS* and *BRAF* mutation status) as well as the type of immunotherapy, the independent prognostic value of this 19-plex MSI signature was confirmed ($HR_{C2} = 13.5$; 95% CI 2.38-76.6; $P = 3.3 \times 10^{-3}$) (Figure 2F).

### *Transcriptomic signatures and response to ICI in MSI mCRC patients*

Previous studies have provided evidence of the predictive value of RNA signature for immunotherapies. Three types of established signatures of response to ICI were systematically assessed in both discovery (C1) and validation (C2) cohorts: signatures quantifying cellular components of the tumor microenvironment ($n = 99$), single gene expression levels ($n = 19\,116$), and signaling pathway activity estimation from gene expression levels ($n = 3365$). None of these established transcriptomic-based signatures could be reproducibly associated to iPFS in the two ICI-treated MSI mCRC cohorts, including those specifically associated to ICI response in previous studies in MSS tumors (e.g. PD-1, programmed death-ligand 1 ± CTLA-4, T or B cells) (Supplementary Figure S4, available at https://doi.org/10.1016/j.annonc.2023.05.010). More specifically, gene sets involved in angiogenesis, epithelial-to-mesenchymal transition, canonical transforming growth factor (TGF)-$\beta$ and Wnt/Wingless signaling pathways, as well as tumor necrosis factor, interferon, KRAS, or mammalian target of rapamycin had either a minor and unreproduced association with iPFS in only one cohort or more generally no significant correlation with survival in any of the two ICI-treated MSI mCRC cohorts (Supplementary Figure S5, available at https://doi.org/10.1016/j.annonc.2023.05.010).

In order to identify context-dependent transcriptomic signatures (i.e. phenotypic descriptors effectively observable in MSI mCRC), an unsupervised blind source separation approach was applied to the transcriptome profiles of the discovery cohort [C1; i.e. independent component analysis (ICA)] (Supplementary Figure S6, available at https://doi.org/10.1016/j.annonc.2023.05.010). Firstly, we considered each ICA and its relevance only in C1 (for all the 10 ICAs), and while 4 had some association with one ICI treatment-related outcome (iRECIST and/or iPFS), only the component with the highest association with iPFS was considered; next, we evaluated the selected component in C2 for the possibility of statistical association with iPFS ($HR_{C1} = 1.87$; 95% CI 1.06-3.3; $P = 0.0282$; $HR_{C2} = 1.75$; 95% CI 1.03-2.98; $P = 0.035$) (Figure 3B and C and Supplementary Figure S6, available at https://doi.org/10.1016/j.annonc.2023.05.010). The RNA component was significantly correlated to an RNA-based quantification of fibroblasts ($P < 0.001$) and anti-correlated to the tumor cellularity ($P < 0.001$) confirming its stromal origin (Figure 3A, Supplementary Table S6, available at https://doi.org/10.1016/j.annonc.2023.05.010, for the list of genes most contributing to this fibrosis component). Besides, Supplementary Figure S7, available at https://doi.org/10.1016/j.annonc.2023.05.010, illustrates the proportion of each consensus molecular subtype (CMS) for each sample in C1.[36] Our fibrosis signature was associated to a tendon-like phenotype, extracellular matrix (ECM)-producing and interacting genes, enriched intratumor CMS4 proportions, and a pan-fibroblast TGF-$\beta$ response signature (PMID: 29443960) (Figure 3A and Supplementary Figure S7, available at https://doi.org/10.1016/j.annonc.2023.05.010). The fibrosis signature was not related to stromal abundance, as measured by Sirius Red staining (Supplementary Figure S8, available at https://doi.org/10.1016/j.annonc.2023.05.010). Exactly as this was previously carried out with the DNA signature, we confirmed the independent prognostic value of this RNA signature using

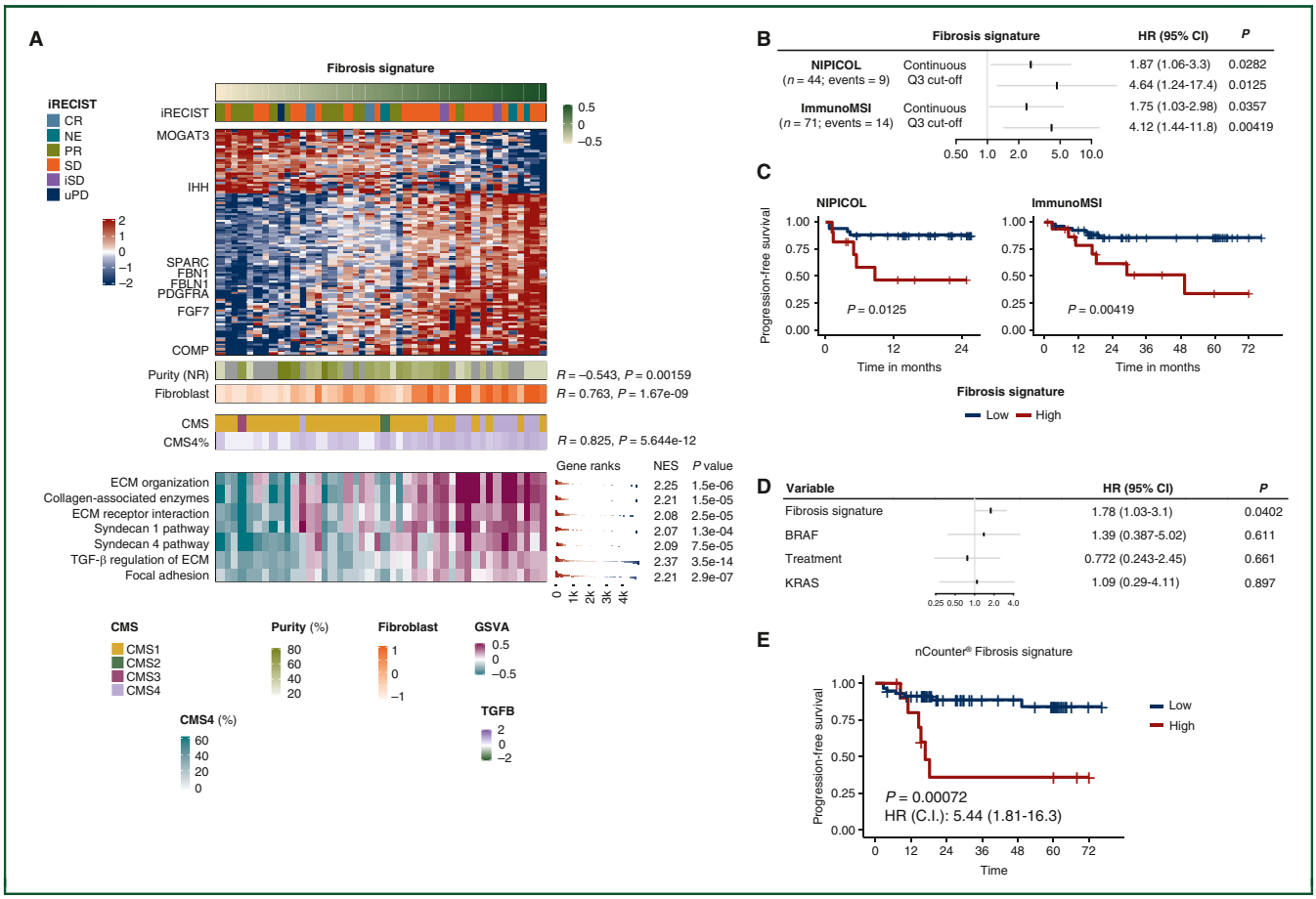


**Figure 3. Transcriptomic signatures and response to ICI in MSI mCRC patients.** (A) Heatmap of the fibrosis signature, patients (in column) are ordered by the estimated quantification of the fibrosis ICA signature. iRECIST status of patients[29] is shown along with gene-wise centered expression values of the gene most associated to the component, tumor purity estimated by the non-repeated variant allele frequency, MCPcounter-based fibroblast quantification estimate, the main consensus molecular subtype (CMS) and the intra-tumoral proportion estimate of CMS4, and TGFB response signature.[40] Pathway-level activity estimate is also shown along with the Gene Set Enrichment Analysis estimates. (B) Univariate association with progression-free survival in the NIPICOL cohort (C1, $n = 44$) or ImmunoMSI (C2, $n = 71$) of the continuous score of the signature or of a classification using the third quartile as a threshold (Q3 cut-off). (C) Kaplan–Meier estimates using the third quantile threshold of the fibrosis signature. (D) Forest plot of the multivariate Cox regression with progression-free survival in cohort C2, representing hazard ratio (HR <1: beneficial, HR = 1: no effect, HR >1: deleterious) with its corresponding *P* value. Included features are fibrosis signature (low to high), BRAF, KRAS (wild type versus mutated), and treatment (mono versus combo). (E) Kaplan–Meier estimates of the nCounter® signature in ImmunoMSI ($n = 69$).
CI, confidence interval; CMS, consensus molecular subtype; CR, complete response; ECM, extracellular matrix; ICI, immune checkpoint inhibitor; iRECIST, immune RECIST; iSD, stable disease by iRECIST; mCRC, metastatic colorectal cancer; MSI, microsatellite instability; NE, not evaluable; PR, partial response; SD, stable disease; TGFB, transforming growth factor beta; TGF-$\beta$, transforming growth factor-$\beta$; uPD, unconfirmed progression disease.

a multivariate analysis in C2 ($HR_{C2} = 1.78$; 95% CI 1.03-3.01; $P = 0.040$) (Figure 3D and Supplementary Table S1, available at https://doi.org/10.1016/j.annonc.2023.05.010). We successfully reduced this RNA signature to a more serviceable set of 182 biomarkers (Supplementary Table S7, available at https://doi.org/10.1016/j.annonc.2023.05.010). Using this raw subpanel, the Spearman correlation with the original component was 0.98 in NIPICOL and 0.96 in ImmunoMSI. Both remained associated with iPFS as continuous scores (Supplementary Figure S9, available at https://doi.org/10.1016/j.annonc.2023.05.010).

### *Transfer to clinical-grade fibrosis signature*

Finally, we wanted to further test the possibility to validate our RNA signature predicting response to ICI in patients with MSI mCRC using an alternative method than 3′ RNASeq. This was done by using a nanoString nCounter® technology (Nanostring) more accessible for routine clinical practice (Supplementary Figure S10, available at https://doi.org/10.1016/j.annonc.2023.05.010). A subset of C1 tumors ($n = 27$) were profiled using a panel of 182 genes from the fibrosis signature on nanoString nCounter®(Nanostring), of which 74 were selected to best match the RNASeq signature. This transferred nCounter® fibrosis signature was applied to C2 (subset, $n = 69$) and showed a significant association with iPFS (Figure 3E).

### *Multivariate analyses combining the DNA and RNA signatures*

We finally examined the effect of both RNA and DNA signatures in predicting iPFS to ICI in MSI mCRC patients using a multivariate model (Figure 4). When taking into account both signatures in either a continuous or a discrete way, the multivariate analysis indicated that both signatures were independently predictive of iPFS (Figure 4A). Figure 4B (and Supplementary Figure S11, available at https://doi.org/10.1016/j.annonc.2023.05.010) shows how these DNA and RNA signatures are complementary and effective when used

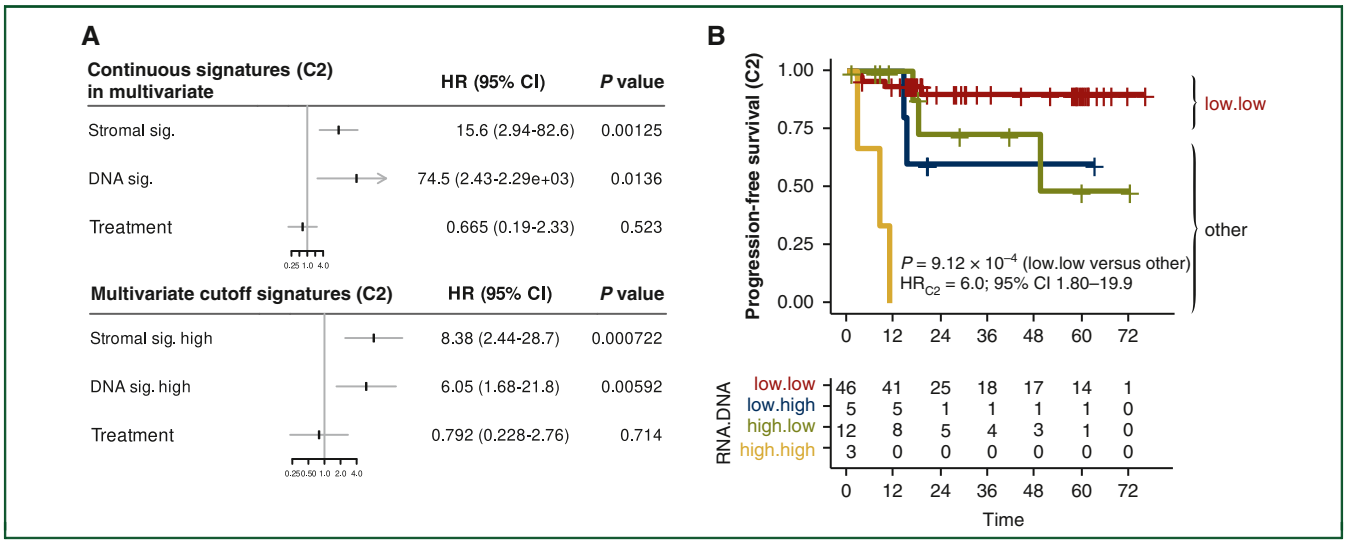


**Figure 4. Multivariate analyses combining the DNA and RNA signatures.** (A) Forest plot displaying the RNA or DNA signatures as well as the treatment type considering either the continuous values (upper panel) or by discretizing the values (lower panel) of the signatures. (B) Kaplan–Meier estimates of progression-free survival (iPFS) based on the intensity combination of the two signatures ($n = 66$). High RNA and DNA signatures are shown in red. Low RNA and DNA signatures are shown in green. High RNA signature and weak DNA signature are shown in orange and low RNA signature and high DNA signature are shown in purple.
CI, confidence interval; HR, hazard ratio; iPFS, progression-free survival by immune RECIST.

together in predicting the response of patients to ICI treatment. One and/or another of the signatures was able to predict progression in patients from C2 regarding iPFS to ICI ($HR_{C2} = 6.0$; 95% CI 1.80-19.9; $P = 9.12 \times 10^{-4}$). This makes these signatures a valuable classifier tool capable of predicting relapse in MSI mCRC patients (see also in Supplementary Figure S9, available at https://doi.org/10.1016/j.annonc.2023.05.010, the performance of this combined analysis when the RNA fibrosis signature was reduced to 182 markers).

## DISCUSSION

In this study, we examine the issue of response to ICI in patients with dMMR/MSI mCRC. ICIs are expected to be highly efficient, with relatively rare progression events, in this population. Although this is fortunate for the general population, it makes crucial the identification of high-risk patients yet hindering statistical analyses in translational studies. This reinforces the importance of our work based on the analysis of two independent prospective cohorts of patients used as discovery and validation sets, which is particularly appropriate from a statistical point of view. Furthermore, this study is limited to CRC patients only, thus avoiding the risk that the origin of the primary tumor might interfere with the results. The dual approach of high-throughput analysis of tumor DNA and RNA enables us to carry out both supervised and unsupervised analyses with the aim of investigating ICI response-associated genotypes and phenotypes in MSI mCRC. Finally, the dMMR/MSI status of the tumors was systematically rechecked in our expert center as part of this ancillary study to avoid misdiagnoses which can deeply impact the findings of such translational research studies, as reported.[24,37] All these points constitute methodological strengths of the present work compared to others in the field which remain few and based on a smaller number and/or more heterogeneous series of patients.

We first show that several previously suggested DNA and RNA indicators are unlikely to have any predictive values regarding response to ICI in MSI mCRC patients. This is primarily the case for the quantitative DNA markers MSI-sensor score and TMB regardless of the cut-off selected for these indexes in survival analyses.[15,16] By contrast, accounting for MSI misdiagnoses (false-positive MSI CRC) drastically changes the predictive value of TMB and MSI-sensor at a low threshold (10th percentile), leading to the incorrect conclusion that these genomic indexes may predict ICI resistance. With respect to this issue, here we very rigorously examine the MSI/dMMR status of all included tumor samples by IHC, MSI-PCR, and NGS, and this point will have to be strictly observed to make conclusions on the real predictive value of these genomic indexes in future studies. In addition, our analyses based on previously defined candidate DNA/RNA markers of resistance, e.g. specific somatic DNA variants, the activity of canonical signaling pathways, or the presence of specific cellular contingents within the tumor bulk, also failed to identify robust predictors of ICI response in patients. Though some of these markers may contribute to some extent to modulate the patients' response to ICI in some dMMR/MSI mCRC as suggested by some studies carried out on smaller series of patients, and more generally may be predictive of ICI efficacy in MMR-proficient tumors, they are unlikely to have major clinical relevance.

The breakthrough results we have achieved in this study stem from the fact that we report and validate in both cohorts two distinct original signatures derived from a global analysis of the DNA and RNA profiles of ICI-treated MSI mCRC. In brief, the DNA signature is epithelial in nature. It analyzes the combination of a 19-plex panel aggregating independent somatic mutational events in dMMR tumor cells involving both coding and noncoding microsatellite-containing genes associated to distinct biological processes. As some

microsatellite mutations such as those in the pentaplex are relevant for MSI diagnosis in CRC, the combined analysis of these 19 microsatellites is of predictive interest for response to ICI as evaluated by iPFS in patients. We have here followed a rigorous methodological approach to highlight the clinical relevance of this DNA signature using two completely independent prospective cohorts of MSI mCRC patients including a training set that was a clinical trial. Understanding this signature and its effect, which is an interesting question, will be the subject of future studies. It is presently difficult to judge the relevance of the microsatellite gene mutations it contains. Their role can be direct but also indirect by being events associated with others more functionally relevant in cancer cells. In addition, the RNA signature is fibrotic in nature. In contrast to CMS which constitutes transcriptomic objects whose use in the clinic is cumbersome due to the juxtaposition of several CMS contingents per tumor,[36] the RNA signature we propose in this study is dedicated to MSI tumors and seems to show a real ability to simply predict response to ICI in this specific subset of CRC at the metastatic stage. Though it is transforming growth factor beta (TGFB)-related with a desmoplastic orientation, the fact that Sirius Red staining does not discriminate between samples with and without this fibrosis signature illustrates its complex nature. Noteworthily, all the previously defined signatures and pathways that were shown to be associated to the proposed transcriptomic-defined TGFB-related fibrosis signature were not themselves associated to progression in both cohorts. This highlights the importance of defining context-dependent signatures, in particular in such distinct carcinogenic and microenvironment context as those found in MSI mCRC. In relation to a rich literature that has already provided evidence that the ECM and its heterogeneous content could promote resistance to ICI in MSS tumor models associated with various primary locations (for review see O'Donnell et al.[38]), the RNA contingent we are identifying could thus play such a role by promoting, for example, immune-exclusion or sequestration processes in the context of increased fibrosis generated in and around the tumor. It could also modulate the response to treatment through non-mutually exclusive mechanisms involving more specifically the cancer-associated fibroblasts hosted in or responsible for the matrix generation.

Our work has some limitations. Firstly, it does not address the issue of the choice of immunotherapy, i.e. monotherapy with anti-PD-1 or combination of anti-PD-1 and anti-CTL4. Secondly, the question of epigenetics is an especially important issue that is not addressed here and will require further investigation in subsequent studies. Thirdly, our work does not really shed light on simple mechanisms underlying resistance to ICI in MSI mCRC. In this respect, it is not yet very enlightening for the identification of novel therapeutic targets that could be of interest in the future for patients with primary or secondary resistance to anti-PD-1 ± anti-CTL4, although the targeting of the tumor microenvironment and the ECM in particular is a very interesting avenue. It will be important to conduct future studies in MSI CRCs that will take into account the clonal complexity of the MSI 'hot' cancer paradigm and their specific microenvironment, considering the question of response to ICIs at the clonal level using geo-spatialization and single cell analyses, as has already been done in other studies not dedicated to this very specific type of cancer.[39] Finally, although our results were established on a large prospective collection of patients including two independent cohorts, one of which is a clinical trial, they still require validation in new populations of metastatic MSI cancer patients, with colorectal tumor but possibly also other primary MSI cancer, and in a preferential way with patients treated with anti-PD-1/PD-L1 alone. Despite these weaknesses, the two signatures we outline here from the analysis of the tumor bulk are easy to investigate and can be implemented in the context of a clinical routine. The DNA signature requires the analysis of the status of only 19 microsatellite markers within the tumor, ideally by NGS but also by other methods while the RNA signature requires to carry out 3′ RNASeq which is a simple, reproducible, and feasible method to be used with paraffin-embedded tumor samples, the cost of which has now decreased considerably. Moreover, the RNA signature can be also investigated using a nanoString nCounter® technology (Nanostring) more accessible for routine clinical practice, even with a smaller number of markers. Finally, it is very interesting to note that the DNA and RNA signatures have independent predictive value and can be used jointly to predict progression in ICI-treated MSI mCRC patients. This should be of interest for the design of future strategies improving ICI for MSI cancer patients in clinics.

## ACKNOWLEDGEMENTS

The authors thank the patients and their families for making the study possible. The authors acknowledge the GERCOR clinical study teams, the IDEATION study group, and investigators and study teams in all centers.

## FUNDING

This work was supported by grants from Site de Recherche Intégré sur le Cancer (SIRIC) Cancer United Research Associating Medicine, University & Society (CURAMUS, Grants Inserm, DGOS and Inserm, period 2018-22, no grant number), and the Ligue Nationale Contre le Cancer (no grant number). TR was a recipient of a grant from the Region Ile-de-France (PhD Student bursary, no grant number). ADu's team has the label de La Ligue contre le Cancer (period 2020-22, no grant number).

## DISCLOSURE

The authors have declared no conflicts of interest.

## REFERENCES

1. Ionov Y, Peinado MA, Malkhosyan S, et al. Ubiquitous somatic mutations in simple repeated sequences reveal a new mechanism for colonic carcinogenesis. *Nature*. 1993;363(6429):558-561.
2. Aaltonen LA, Peltomaki P, Leach FS, et al. Clues to the pathogenesis of familial colorectal cancer. *Science*. 1993;260(5109):812-816.
3. Fishel R, Lescoe MK, Rao MR, et al. The human mutator gene homolog MSH2 and its association with hereditary nonpolyposis colon cancer. *Cell*. 1993;75(5):1027-1038.

4. Svrcek M, Lascols O, Cohen R, et al. MSI/MMR-deficient tumor diagnosis: which standard for screening and for diagnosis? Diagnostic modalities for the colon and other sites: differences between tumors. *Bull Cancer*. 2019;106(2):119-128.
5. Hamelin R, Chalastanis A, Colas C, et al. [Clinical and molecular consequences of microsatellite instability in human cancers]. *Bull Cancer*. 2008;95(1):121-132.
6. Duval A, Hamelin R. Mutations at coding repeat sequences in mismatch repair-deficient human cancers: toward a new concept of target genes for instability. *Cancer Res*. 2002;62(9):2447-2454.
7. Llosa NJ, Cruise M, Tam A, et al. The vigorous immune microenvironment of microsatellite instable colon cancer is balanced by multiple counter-inhibitory checkpoints. *Cancer Discov*. 2015;5(1):43-51.
8. Le DT, Uram JN, Wang H, et al. PD-1 blockade in tumors with mismatch-repair deficiency. *N Engl J Med*. 2015;372(26):2509-2520.
9. Cohen R, Colle R, Pudlarz T, et al. Immune checkpoint inhibition in metastatic colorectal cancer harboring microsatellite instability or mismatch repair deficiency. *Cancers (Basel)*. 2021;13(5):1149.
10. Andre T, Shiu KK, Kim TW, et al. Pembrolizumab in microsatellite-instability-high advanced colorectal cancer. *N Engl J Med*. 2020;383(23):2207-2218.
11. Le DT, Durham JN, Smith KN, et al. Mismatch repair deficiency predicts response of solid tumors to PD-1 blockade. *Science*. 2017;357(6349):409-413.
12. Overman MJ, McDermott R, Leach JL, et al. Nivolumab in patients with metastatic DNA mismatch repair-deficient or microsatellite instability-high colorectal cancer (CheckMate 142): an open-label, multicentre, phase 2 study. *Lancet Oncol*. 2017;18(9):1182-1191.
13. Overman MJ, Lonardi S, Wong KYM, et al. Durable clinical benefit with nivolumab plus ipilimumab in DNA mismatch repair-deficient/microsatellite instability-high metastatic colorectal cancer. *J Clin Oncol*. 2018;36(8):773-779.
14. Cohen R, Bennouna J, Meurisse A, et al. RECIST and iRECIST criteria for the evaluation of nivolumab plus ipilimumab in patients with microsatellite instability-high/mismatch repair-deficient metastatic colorectal cancer: the GERCOR NIPICOL phase II study. *J Immunother Cancer*. 2020;8(2):e001499.
15. Mandal R, Samstein RM, Lee KW, et al. Genetic diversity of tumors with mismatch repair deficiency influences anti-PD-1 immunotherapy response. *Science*. 2019;364(6439):485-491.
16. Schrock AB, Ouyang C, Sandhu J, et al. Tumor mutational burden is predictive of response to immune checkpoint inhibitors in MSI-high metastatic colorectal cancer. *Ann Oncol*. 2019;30(7):1096-1103.
17. Gurjao C, Liu D, Hofree M, et al. Intrinsic resistance to immune checkpoint blockade in a mismatch repair-deficient colorectal cancer. *Cancer Immunol Res*. 2019;7(8):1230-1236.
18. Chida K, Kawazoe A, Suzuki T, et al. Transcriptomic profiling of MSI-H/dMMR gastrointestinal tumors to identify determinants of responsiveness to anti-PD-1 therapy. *Clin Cancer Res*. 2022;28(10):2110-2117.
19. Kwon M, An M, Klempner SJ, et al. Determinants of response and intrinsic resistance to PD-1 blockade in microsatellite instability-high gastric cancer. *Cancer Discov*. 2021;11(9):2168-2185.
20. Bortolomeazzi M, Keddar MR, Montorsi L, et al. Immunogenomics of colorectal cancer response to checkpoint blockade: analysis of the KEYNOTE 177 trial and validation cohorts. *Gastroenterology*. 2021;161(4):1179-1193.
21. Chida K, Kawazoe A, Kawazu M, et al. A low tumor mutational burden and PTEN mutations are predictors of a negative response to PD-1 blockade in MSI-H/dMMR gastrointestinal tumors. *Clin Cancer Res*. 2021;27(13):3714-3724.
22. Latham A, Srinivasan P, Kemel Y, et al. Microsatellite instability is associated with the presence of Lynch syndrome pan-cancer. *J Clin Oncol*. 2019;37(4):286-295.
23. Germano G, Lu S, Rospo G, et al. CD4 T cell-dependent rejection of beta-2 microglobulin null mismatch repair-deficient tumors. *Cancer Discov*. 2021;11(7):1844-1859.
24. Cohen R, Hain E, Buhard O, et al. Association of primary resistance to immune checkpoint inhibitors in metastatic colorectal cancer with misdiagnosis of microsatellite instability or mismatch repair deficiency status. *JAMA Oncol*. 2019;5(4):551-555.
25. Colle R, Radzik A, Cohen R, et al. Pseudoprogression in patients treated with immune checkpoint inhibitors for microsatellite instability-high/mismatch repair-deficient metastatic colorectal cancer. *Eur J Cancer*. 2021;144:9-16.
26. Buhard O, Cattaneo F, Wong YF, et al. Multipopulation analysis of polymorphisms in five mononucleotide repeats used to determine the microsatellite instability status of human tumors. *J Clin Oncol*. 2006;24(2):241-251.
27. Buhard O, Lagrange A, Guilloux A, et al. HSP110 T17 simplifies and improves the microsatellite instability testing in patients with colorectal cancer. *J Med Genet*. 2016;53(6):377-384.
28. Ratovomanana T, Cohen R, Svrcek M, et al. Performance of next-generation sequencing for the detection of microsatellite instability in colorectal cancer with deficient DNA mismatch repair. *Gastroenterology*. 2021;161(3):814-826 e817.
29. Seymour L, Bogaerts J, Perrone A, et al. iRECIST: guidelines for response criteria for use in trials testing immunotherapeutics. *Lancet Oncol*. 2017;18(3):e143-e152.
30. Boegel S, Lower M, Schafer M, et al. HLA typing from RNA-Seq sequence reads. *Genome Med*. 2012;4(12):102.
31. Hundal J, Kiwala S, McMichael J, et al. pVACtools: a computational toolkit to identify and visualize cancer neoantigens. *Cancer Immunol Res*. 2020;8(3):409-420.
32. Lundegaard C, Lamberth K, Harndahl M, et al. NetMHC-3.0: accurate web accessible predictions of human, mouse and monkey MHC class I affinities for peptides of length 8-11. *Nucleic Acids Res*. 2008;36:W509-W512. Web Server issue).
33. Reynisson B, Alvarez B, Paul S, et al. NetMHCpan-4.1 and NetMHCIIpan-4.0: improved predictions of MHC antigen presentation by concurrent motif deconvolution and integration of MS MHC eluted ligand data. *Nucleic Acids Res*. 2020;48(W1):W449-W454.
34. Wang J, Xiu J, Farrell A, et al. Mutational analysis of microsatellite-stable gastrointestinal cancer with high tumour mutational burden: a retrospective cohort study. *Lancet Oncol*. 2023;24(2):151-161.
35. Abraham A, Pedregosa F, Eickenberg M, et al. Machine learning for neuroimaging with scikit-learn. *Front Neuroinform*. 2014;8:14.
36. Marisa L, Blum Y, Taieb J, et al. Intratumor CMS heterogeneity impacts patient prognosis in localized colon cancer. *Clin Cancer Res*. 2021;27(17):4768-4780.
37. Loupakis F, Depetris I, Biason P, et al. Prediction of benefit from checkpoint inhibitors in mismatch repair deficient metastatic colorectal cancer: role of tumor infiltrating lymphocytes. *Oncologist*. 2020;25(6):481-487.
38. O'Donnell JS, Teng MWL, Smyth MJ. Cancer immunoediting and resistance to T cell-based immunotherapy. *Nat Rev Clin Oncol*. 2019;16(3):151-167.
39. Litchfield K, Reading JL, Puttick C, et al. Meta-analysis of tumor- and T cell-intrinsic mechanisms of sensitization to checkpoint inhibition. *Cell*. 2021;184(3):596-614.e514.
40. Powles T, Kockx M, Rodriguez-Vida A, et al. Clinical efficacy and biomarker analysis of neoadjuvant atezolizumab in operable urothelial carcinoma in the ABACUS trial. *Nat Med*. 2019;25(11):1706-1714.